Journal of Thermal Analysis and Calorimetry (2023) 148:1373–1379
https://doi.org/10.1007/s10973-022-11844-0

Thermoanalytic characterization of binder burnout and sintering of lead-free piezoelectric KNNLT multilayer laminates with Ni electrodes

M. W. Alkanj[1] · A. Kynast[2] · M. Töpfer[2] · F. Schubert[2] · J. Töpfer[1]

Received: 31 March 2022 / Accepted: 27 November 2022 / Published online: 10 January 2023

Abstract
For competitive lead-free piezoceramic multilayer actuators (MLA) it is required to include base metal electrodes (BMEs). However, thermal processing of KNN-based multilayers with Ni electrodes necessitates precise control of the oven atmosphere in order to control the phase composition and functional performance of the piezoceramics and electrodes. Sintering of KNN-based MLAs with BMEs is performed at low oxygen partial pressure followed by a reoxidation treatment to reduce the concentration of oxygen vacancies and increase the resistivity of the ferroelectric, and simultaneously, the BME must not be oxidized. Within this complex thermal treatment protocol, the debindering of the multilayer laminates is a very important process step and proper binder removal is critical to avoid formation of defects or flaws and oxidation of electrodes. We have studied the debindering behavior of a KNN-based MLA with Ni electrodes fabricated from a PVB-based slip formulation using thermal analysis and complementary binder burnout experiments under reducing atmospheres. It is shown that binder burnout in reducing atmosphere allows for protection of Ni layers, but incomplete binder decomposition occurs at lower p_{O2}. On the other hand, after debindering at 350 °C in air complete binder removal and little Ni oxidation only was observed, allowing to use these binder burnout conditions to prepare MLAs.

Keywords Lead-free piezoelectric materials · Sodium potassium niobate · Multilayer actuators · Reduced atmosphere · Binder burnout

Introduction

Perovskites of the $Pb(Zr,Ti)O_3$ (PZT) system represent the materials basis for a tremendous variety of piezoelectric applications [1]. However, due to environmental concerns and the toxicity of lead as major constituent, alternative lead-free piezoceramics are intensively studied [2]. To date, transformation into industry-scale fabrication technology and application market penetration remain challenging [3]. Piezoelectric multilayer actuators (MLA) are electronic devices which allow for transformation of electric signals into nanometer to micrometer displacements with low-voltage driving. They are used for many applications including automotive injection or precision positioning systems. Large interest in potassium-sodium niobate (KNN)-based multilayer devices evolved recently. It was shown that the fabrication of MLAs by cofiring of Li- and (Ta, Sb)-modified sodium potassium niobate (KNNLT) and AgPd (70/30) inner electrodes is possible [4, 5]. The use of base metals electrodes (BME) in MLAs is a new and challenging issue, but it is urgently needed to reduce actuator costs. However, in that case sintering of MLAs needs to be carried out under reducing atmosphere to avoid oxidation of the Ni electrode during cofiring [6]. Typically, during sintering at low oxygen partial pressure densification and microstructure formation take place under conditions of thermodynamic stability of the base metal electrode and piezoceramics. The significant concentration of oxygen vacancies, formed in the KNN lattice at high temperature and low p_{O2} is reduced in the subsequent reoxidation treatment giving rise to an increase of the insulation resistance of the piezoceramic layers. However, it is necessary to control the oxidation kinetics

✉ J. Töpfer
joerg.toepfer@eah-jena.de

[1] Department SciTec, Ernst-Abbe-Hochschule Jena, C.-Zeiss-Promenade 2, 07745 Jena, Germany

[2] PI Ceramic GmbH, Lindenstraße, 07589 Lederhose, Germany

of the Ni electrodes and to avoid deterioration of electrode functionality. So far, the fabrication of a 12-layer actuator using modified KNN cofired with Ni electrodes under low oxygen partial pressure was demonstrated, and a normalized piezoelectric coefficient of d^*_{33}= 360 pm/V was obtained [7]. Cofiring of KNN with Ni electrodes [8] and reducing atmosphere sintering of KNN [9], $NaNbO_3$ [10], and KNNLT [11] were reported. Cofiring of KNNLT multilayer actuators with Cu inner electrodes at 1050 °C and $p_{O2} = 10^{-10}$ atm and reoxidation treatment at 850 °C and $p_{O2} = 10^{-5}$ atm was proposed as well [12].

The multilayer process for the fabrication of MLAs is based on KNN green tapes made by tape casting using a slurry that consists of the piezoceramic powder dispersed in solvents, together with binders, plasticizers and dispersants. After printing of electrodes and stacking, the thermal process of debindering is carried out in order to remove all organic materials from the green tapes as prerequisite for subsequent sintering steps. Standard green tapes typically contain polyvinyl butyral (PVB) binders which are burned out at approximately 450 °C in air. Binder burnout of PVB proceeds via removal of water, elimination of side groups, and formation of unsaturated organic chains [13]. In the case of use of BMEs, however, binder burnout in air atmosphere at high temperatures may lead to potential oxidation of the electrode. Instead, green tapes with printed BME electrodes require individual debindering schedules and smart sintering and reoxidation protocols. The binder removal in PVB-based green tape formulations for multilayer ceramic capacitors (MLCC) with base metal electrodes has been studied two decades ago and is well established nowadays in the fabrication of BME MLCCs. It was shown that the initial stage of binder removal occurs at the interface between electrodes and dielectric layers and leads to maximum deformation. It was concluded that low heating rates are required in that early stage of binder burnout [14]. The debindering of a slip system with PVB binder in nitrogen was studied as well, and decomposition of the binder is finished at about 400 °C [15]. The effects of the burnout parameters on the binder removal and microstructure in $BaTiO_3$-based Ni-MLCCs with X7R characteristic have been investigated [16]. Ambient atmosphere was more effective in removing the binder than nitrogen atmosphere; however, delamination took place at faster heating rate in ambient conditions. Another problem that might arise is incomplete binder burnout and formation of carbon residues which might deteriorate the functional performance of the device [17]. Alternative binder systems for thermal decomposition at low temperature in air or nitrogen atmosphere based on polypropylene carbonate were also proposed [18].

We report here on thermoanalytic investigations of the binder burnout behavior of PVB-based KNNLT green tapes with Ni electrodes. The thermal decomposition of the binder was studied for different oxygen partial pressures. Complementary studies of the debindering process in different atmospheres were performed in a tube furnace equipped with p_{O2} sensors which allows in situ observations of oxygen uptake or release. We also report on phase compositions of the KNNLT-based multilayer components after binder burnout and after sintering/reoxidation under reduced p_{O2}.

Experimental

The multilayer laminates were fabricated using tape casting with a doctor-blade. The casting slurry was made of a Li- and Ta-modified KNN powder of composition close to $K_{0.48}Na_{0.48}Li_{0.04}Nb_{0.80}Ta_{0.20}O_3$ and a polyvinyl butyral (PVB)-based binder system. Electrodes were printed with a commercial Ni-paste. Ten layers of green tapes with thickness of about 100 µm were stacked and laminated at 70–80 °C and 20–30 MPa with size 12 * 12 mm^2.

The binder burnout was monitored using Setaram TGA 92 (DTA) and TAG 24 (TG) thermal analysis systems as well as in a tube furnace, all equipped with mass flow controller-based O_2/N_2 gas mixing systems to generate different oxygen partial pressures. Both, the TG /DTA systems and the tube furnace were coupled to a zirconia-based p_{O2} measuring system at the exit of the gas streams. For thermal analysis, multilayer samples without and with Ni electrodes were heated with 2 K min^{-1} to the final debindering temperature T_{db} and held there for several hours in a gas atmosphere with a defined p_{O2}. For binder burnout experiments in the tube furnace, the samples were heated initially with 0.4 K min^{-1} to 100 °C and then with 0.06 K min^{-1} to T_{db}. Finally, some multilayer actuators were annealed in a muffle furnace for binder burnout to 350 °C in air with a heating rate of 0.06 K min^{-1}. Sintering of the MLAs was performed at 1000 °C for 1 h at an oxygen partial pressure of 10^{-10} atm, and reoxidation at 850 °C for 12 h at p_{O2} of 10^{-6} atm in a tube furnace with a gas atmosphere established using a gas mixing unit and mixtures of dry nitrogen, Ar/H_2 (95/5) forming gas, and saturated wet N_2 gas (30 °C).

The samples were examined using an optical microscope (AXIO Imager.A2m, Carl Zeiss AG). The phase formation was investigated using X-ray diffraction (D8 ADVANCE, Cu-K_α radiation, Bruker AXS, Karlsruhe, Germany) on crushed debindered powder samples and on cross sections of polished sintered multilayer samples. Measurements of the dielectric and electromechanical properties were taken with an impedance analyzer (Agilent Impedance Analyzer-4294 A, Agilent Technologies Inc.). Unipolar displacement measurements were taken with a TF analyzer (aixACCT Systems GmbH, Aachen), and the normalized strain coefficient $d^*_{33} = S_{max}/E_{max}$ was calculated for $E = 3$ kV mm^{-1}.

Results and discussion

The thermoanalytical investigations were started with the pure PVB binder system (Fig. 1). The decomposition in an atmosphere with an oxygen partial pressure of $p_{O2} = 10^{-1}$ atm (which is close to that of air) shows a mass loss starting at about 250 °C, reaching its peak at about 335 °C and persisting up to 480 °C. Simultaneously, a peak in the p_{O2} signal of the surrounding gas atmosphere appears at 335 °C, indicating consumption of oxygen from the gas atmosphere for oxidation of binder components. If the same experiment is performed at $p_{O2} = 10^{-3}$ atm, the decomposition of the binder proceeds in a somewhat shorter temperature range and is finished already at 400 °C. In this case, the very broad and deep peak in the p_{O2} curve indicates that almost all oxygen from the gas atmosphere is consumed for binder oxidation. This is consistent with results from Sallam et al. [19], who showed that the mass loss upon thermal decomposition of PVB in Ar is finished at 420 °C as compared to 450 °C in air. This is interpreted by two different decomposition pathways of PVB pyrolysis. PVB decomposition in air was shown to form a char residue which needs high temperatures of 750 °C to be completely burned off. This is not the case if decomposition is performed in inert atmosphere [19]. This is confirmed in our experiments: whereas decomposition in 10^{-3} atm leads to a mass loss of 100% at 600 °C and a completely empty crucible, a mass loss of 99.9% and some dark residue in the crucible is found after heating in 10^{-1} atm.

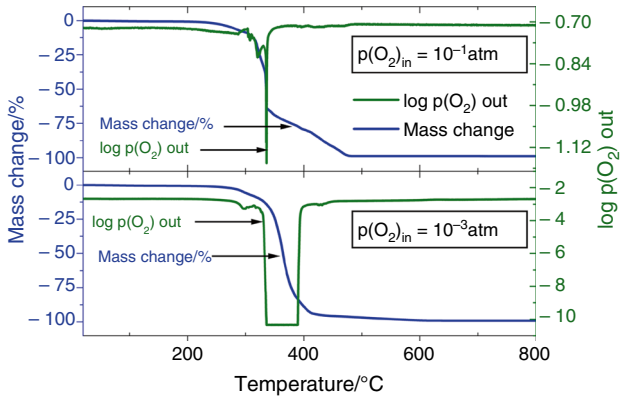

Fig. 1 Thermal analysis of pure PVB binder system (mass change and p_{O2} in the gas atmosphere) during heating with 2 K min^{-1} to 800 °C in $pO_2 = 10^{-1}$ atm (top) and 10^{-3} atm (bottom)

The binder burnout behavior of the KNNLT green tapes was also investigated using thermal analysis. As an example, the thermal effects during heating up to 350 °C in a gas atmosphere with $p_{O2} = 10^{-1}$ atm are shown in detail in Fig. 2

The mass loss starts during the heating segment at 175 °C and is finished 30 min after the final temperature of 350 °C is reached. The earlier start of binder decomposition in the presence of metal oxides due to a catalytic effect has already been reported [17, 20]. The observed mass loss is accompanied by a large exothermal signal at 300 °C. Simultaneously, the oxygen partial pressure in the gas atmosphere drops from its initial value of log $p_{O2} = -0.9$, indicating consumption of oxygen from the gas for combustion of organic components. The p_{O2} reaches its initial level again at the beginning of the dwell period, when the mass loss and the decomposition reactions are finished. This thermoanalytical study implies that the PVB binder in the KNNLT green tape is removed after 1 h at 350 °C at 10^{-1} atm.

The debindering behavior of the KNNLT green tapes was also studied at lower p_{O2}. The obtained mass changes for debindering temperatures of $T_{db} = 400$ °C and 350 °C in different gas atmospheres are shown in Fig. 3. For experiments

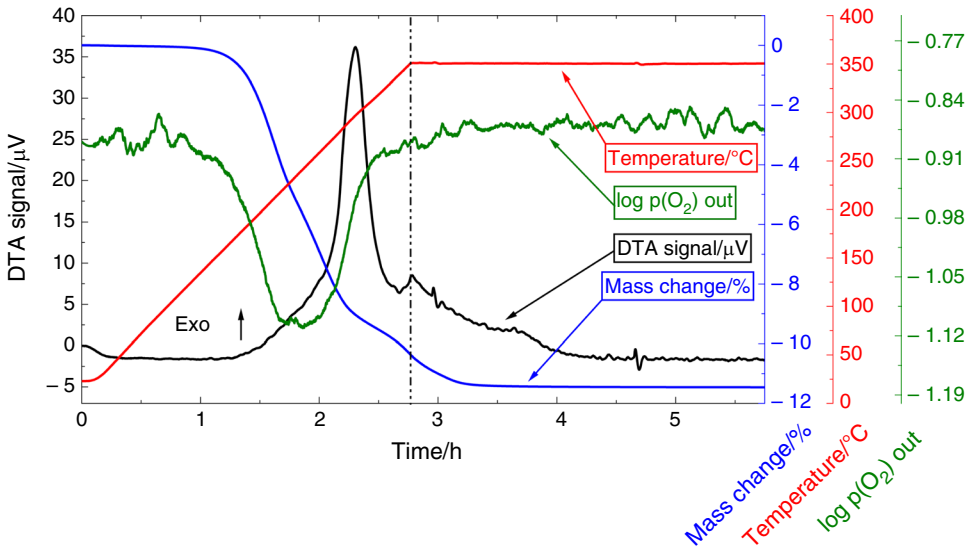

Fig. 2 Thermal analysis of KNNLT green tape (DTA signal, mass change and p_{O2} in the gas atmosphere) during heating with 2 K min^{-1} to 350 °C and dwell of 3 h at 350 °C in $p_{o2} = 10^{-1}$ atm

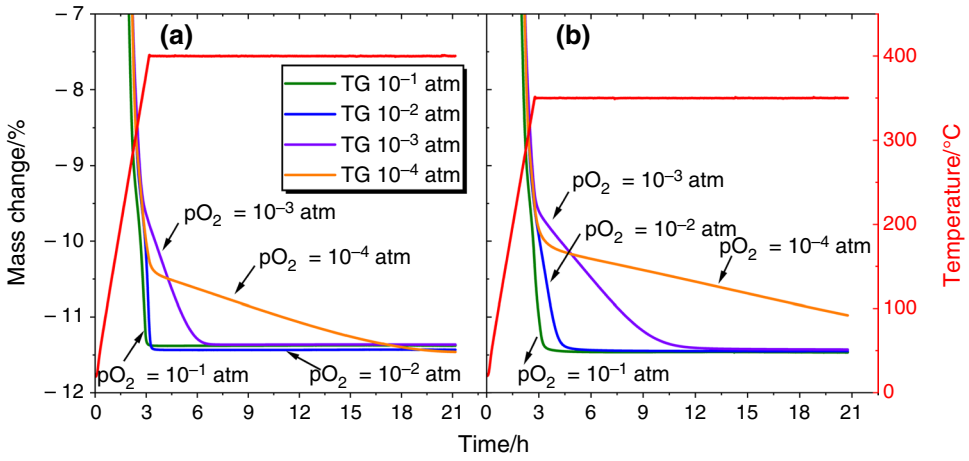

Fig. 3 Thermal analysis of KNNLT green tape (mass change) during heating with 2 K min^{-1} to 400 °C **a** and 350 °C **b** and dwell of 18 h in gas atmospheres with different p_{O2}

performed in a gas atmosphere with $p_{O2} = 10^{-1}$ atm, the mass loss due to PVB decomposition is finished right after the debindering temperatures of $T_{db} = 400$ °C or 350 °C, respectively, are reached. In $p_{O2} = 10^{-2}$ atm a slight shift of the end of binder burnout to somewhat longer dwell times is observed. However, in gas atmospheres with $p_{O2} = 10^{-3}$ atm and $p_{O2} = 10^{-4}$ atm significantly longer dwells at T_{db} are needed for reaching the end of the decomposition. This effect is more pronounced at a lower $T_{db} = 350$ °C; here the debindering process in $p_{O2} = 10^{-4}$ atm is not finished even after a dwell time of 18 h (Fig. 3b).

Finally, the debindering behavior of KNNLT multilayer chips with Ni electrodes was studied using thermal analysis (Fig. 4). The mass change during heating and dwell at $T_{db} = 400$ °C (Fig. 4a) and $T_{db} = 350$ °C (Fig. 4b) is shown for different oxygen partial pressures in the gas atmospheres. In both cases the following features are observed: (i) if the p_{O2} is reduced, longer dwell times are needed to reach the initial mass loss for binder decomposition, and (ii) a slight increase in mass occurs as a second step following the binder decomposition during the dwell at a given T_{db}, and this mass gain increases under more oxidizing conditions. This observed mass gain is a clear indication of partial oxidation of the Ni electrodes during binder burnout. The tendency toward oxidation of Ni increases with higher debindering temperatures, as shown for a gas atmosphere with $p_{O2} = 10^{-1}$ atm in Fig. 4c. It is found that under these conditions significant oxidation of Ni electrodes takes place if the binder burnout is performed at 400 °C or 450 °C, whereas at $T_{db} = 350$ °C a small mass gain is observed indicating very little tendency toward electrode oxidation.

Binder burnout experiments in different atmospheres were performed in a tube furnace equipped with an oxygen sensor to monitor the variation of p_{O2} during the debindering process (Fig. 5). In these experiments the samples were slowly heated to the final debindering temperature and held there for several hours. For debindering in $p_{O2} = 10^{-2}$ atm at 350 °C two peaks are observed in the p_{O2}-curves (Fig. 5a) as

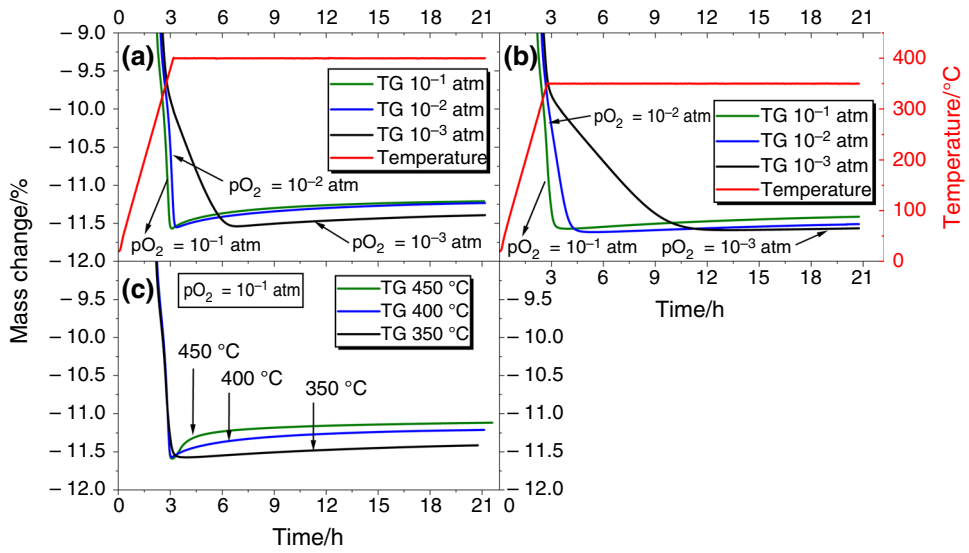

Fig. 4 Thermal analysis of KNNLT-Ni MLAs (mass change) during heating with 2 K min^{-1} to 400 °C **a** and 350 °C **b** and dwell of 18 h in gas atmospheres with different p_{O2}, and in $pO_2 = 10^{-1}$ atm for debindering temperatures of 350 °C, 400 °C, and 450 °C **c**

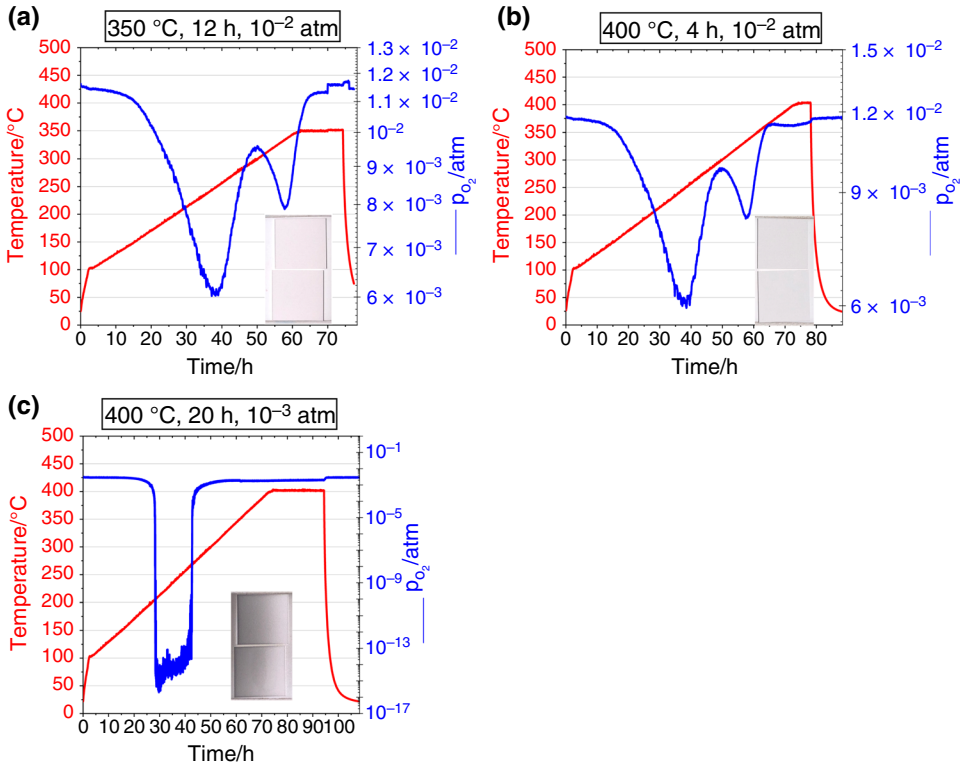

Fig. 5 Binder burnout of KNNLT-Ni MLAs in tube furnace (T and p_{O2} in the gas atmosphere) during heating with 0.4 K min^{-1} to 350 °C in $p_{O2} = 10^{-2}$ atm **a** to 350 °C in $p_{O2} = 10^{-2}$ atm **b** and to 400 °C in in $p_{O2} = 10^{-3}$ atm; insets: photographs of samples after binder burnout

fingerprint of two different binder decomposition processes. However, at the beginning of the dwell the binder burnout is finished and, correspondingly, the initial $p_{O2} = 10^{-2}$ atm is observed. The total mass loss of 11.61% was found and the samples exhibit whitish color. If the binder burnout is performed at 400 °C and $p_{O2} = 10^{-2}$ atm, the corresponding T-p_{O2}-t protocol (Fig. 5b) is very similar. However, the total mass loss is only 11.45% which is a clear indication of partial Ni electrode oxidation. Binder burnout at 400 °C in $p_{O2} = 10^{-3}$ atm proceeds differently: during the heating period the oxygen partial pressure is lowered from 10^{-3} atm by several orders of magnitude to reach values as low as 10^{-13} atm. Obviously, the small supply of oxygen in the atmosphere is needed for binder oxidation reactions, and a different mechanism of binder burnout is active at low oxygen partial pressure (as discussed above). The total mass loss of 11.16% and the dark sample color indicate incomplete binder burnout with formation of residual carbon. A complementary binder burnout experiment was performed at 350 °C in air, and a mass loss of 11.7% and a bright sample color was observed. The residual carbon concentration of these samples was found to amount to 0.06%.

Finally, the phase composition of the debindered samples was studied using XRD. Ni was found in all samples next to reflexes of the majority KNNLT perovskite phase (Fig. 6). However, peaks of NiO were observed in the samples debindered at 400 °C. This is clear experimental proof that partial Ni electrode oxidation takes place at that

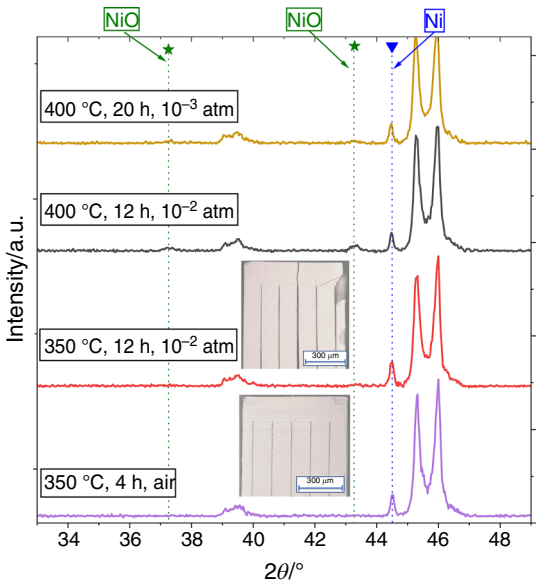

Fig. 6 XRD of powdered KNNLT-Ni MLA samples after binder burnout at different temperatures and p_{O2}; insets: micrographs of MLA samples after binder burnout

temperature, even under slightly reduced p_{O2}. For samples heated to 350 °C in 10^{-2} atm or in air, no peaks of NiO were observed. Closer inspection of the samples debindered at 350 °C in $p_{O2} = 10^{-2}$ atm revealed some cracks at the edges at the electrodes of the multilayer samples (Fig. 6, inset).

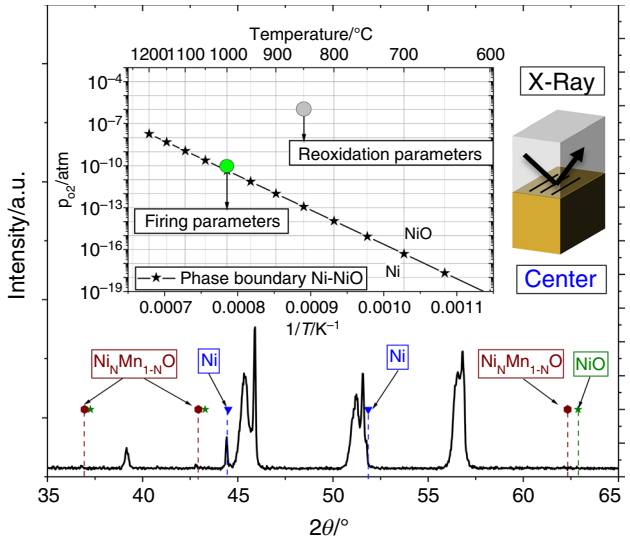

Fig. 7 XRD of sintered KNNLT-Ni MLA sample; inset: Ellingham diagram with Ni/NiO phase boundary, and schematic view of the cross section of the MLA used for XRD analysis

Such cracks were not found in samples after binder burnout at 350 °C in air.

Finally, MLAs with Ni electrodes were debindered at 350 °C in air and sintered at 1000 °C in reduced oxygen partial pressure of 10^{-10} atm and reoxidized at 850 °C and 10^{-6} atm. The phase composition of these sintered samples was inspected using XRD (Fig. 7). The phase boundary of Ni/NiO as Ellingham diagram [21] is included in Fig. 7. Sintering is performed at the phase boundary at 1000 °C to protect the Ni electrodes during sintering. Reoxidation takes place within the Ni phase field underlining the importance of tailoring the reoxidation kinetics of the multilayer samples. The electrode layers were found to mainly consist of Ni metal; however, some oxidation and Ni oxide formation is observed. It is interesting to note that NiO formed at the electrode/ceramics interface seems to absorb some of the Mn dopant to form a $Ni_{1-x}Mn_xO$ solid solution. Details of electrode oxidation and its effect on the device performance will be published somewhere else. Unipolar strain measurements of the sintered multilayer actuators show a strain of about 0.64 ‰ at 3 kV mm^{-1}, an effective coupling factor of $k_{eff} = 0.23$, and the corresponding normalized strain coefficients calculated for the maximum applied field of 3 kV/m is $d^*_{33} = 216$ pm/V.

Conclusions

The binder burnout in KNNLT multilayer laminates and Ni MLAs was investigated using thermal analysis and debindering experiments. Thermal analysis revealed that PVB binder decomposition in KNNLT green tapes is finished at lower temperatures as compared to pure binder. Detailed investigations using different debindering temperatures and oxygen partial pressures were performed to shed light onto the binder burnout process. Thermal decomposition of the PVB binder is also possible at lower p_{O2}, but requires longer dwell times at the debindering temperature T_{db}. At $T_{db} = 350$ °C binder burnout at atmospheres with $p_{O2} < 10^{-2}$ atm is very slow and hence not realistic for complex sample geometries. Debindering of MLAs with Ni electrodes, on the other hand, is characterized by a mass gain indicating electrode oxidation following the initial binder decomposition. This mass gain is the larger, the higher the debindering temperature and the more oxidizing the atmosphere.

Debindering studies in a tube furnace at low $p_{O2} < 10^{-2}$ atm and $T_{db} > 350$ °C result in incomplete binder burnout and/or electrode oxidation. Binder burnout performed by annealing with low heating rate to 350 °C in air was shown to be effective in providing complete binder burnout with low levels of residual carbon and electrode oxidation. Sintered multilayer actuators with inner Ni electrodes exhibit satisfactory performance with $d^*_{33} = 216$ pm/V. However, precise experimental debindering conditions of heating rate, T_{db} and p_{O2} should be determined for each tape slip composition and multilayer geometry. Furthermore, sintering conditions, anisotropic reoxidation kinetics, defect chemistry, and details of electrode oxidation and interaction with ceramic components need to be investigated in detail in order to successfully manage the subtle challenges of lead-free piezoelectric actuator fabrication with base metal electrodes.

Acknowledgements This work was financially supported by the Carl-Zeiss-Stiftung, Germany (P2018-03-001).

Author contributions Conceptualization was contributed by JT; Methodology was contributed by MWA; Formal analysis and investigation were contributed by MWA, AK, and MT; Writing—original draft preparation was contributed by MWA and JT; Writing—review and editing was contributed by JT; Funding acquisition was contributed by JT; Resources were contributed by JT, FS, MT, and AK; Supervision was contributed by JT

Funding Open Access funding enabled and organized by Projekt DEAL.

Declarations

Conflict of interests The authors have no relevant financial or non-financial interests to disclose.

References

1. Jaffe B, Cook WR, Jaffe H Piezoelectric Ceramics, Academic Press, 1971.
2. Rödel J, Jo W, Seifert KTP, Anton EM, Granzow T, Damjanovic D. Perspective on the development of lead-free piezoceramics. J Am Ceram Soc. 2009;92:1153–77. https://doi.org/10.1111/j.1551-2916.2009.03061.x.
3. Rödel J, Webber KG, Dittmer R, Jo W, Kimura M, Damjanovic D. Transferring lead-free piezoelectric ceramics into applications. J Europ Ceram Soc. 2015;35:1659–81. https://doi.org/10.1016/j.jeurceramsoc.2014.12.013.
4. Kim MS, Jeon S, Lee DS, Jeong SJ, Song JS. Lead-free NKN-5LT piezoelectric materials for multilayer ceramic actuator. J Electroceram. 2009;23:372–5. https://doi.org/10.1007/s10832-008-9470-x.
5. Gao R, Chu X, Huan Y, Wang X, Li L. Investigation on cofired multilayer KNN-based lead-free piezoceramics. Phys Stat Sol. 2014;A211:2378–83. https://doi.org/10.1002/pssa.201431156.
6. Gao L, Guo H, Zhang S, Randall CA. Base metal cofired multilayer piezoelectrics. Actuators. 2016;5:8. https://doi.org/10.3390/act5010008.
7. Kawada S, Kimura M, Higuchi Y, Takagi H. "(K, Na)NbO_3-based multilayer piezoelectric ceramics with nickel inner electrodes. Appl Phys Exp. 2009;2: 111401. https://doi.org/10.1143/apex.2.111401.
8. Kobayashi K, Doshida Y, Mizuno Y, Randall CA. Possibility of Cofiring a nickel inner electrode in a ($Na_{0.5}$ $K_{0.5}$)NbO_3–LiF piezoelectric actuator. Jap J Appl Phys. 2013;52(9S1):09KD07. https://doi.org/10.7567/JJAP.52.09KD07.
9. Kobayashi K, Doshida Y, Mizuno Y, Randall CA. A route forwards o narrow the performance gap between PZT and lead-free piezoelectric ceramic with low oxygen partial pressure processed $Na_{0.5}K_{0.5}$NbO3". J Am Ceram Soc. 2012;95:2928–33.
10. Shimizu H, Kobayashi K, Mizuno Y, Randall CA. Advantages of low partial pressure of oxygen processing of alkali niobate: $NaNbO_3$. J Am Ceram Soc. 2014;97:1791–6. https://doi.org/10.1111/jace.12815.
11. Reimann T, Fröhlich S, Bochmann A, Kynast A, Töpfer M, Hennig E, Töpfer J. Low pO2 sintering and reoxidation of lead-free KNNLT piezoceramic laminates. J Europ Ceram Soc. 2021;41:344–51. https://doi.org/10.1016/j.jeurceramsoc.2020.07.066.
12. Gao L, Ko SW, Guo H, Hennig E, Randall CA. Demonstration of Copper cofired (Na, K)Nb_O3 multilayer structures for piezoelectric applications. J Am Ceram Soc. 2016;99:2017–23. https://doi.org/10.1111/jace.14207.
13. Lewis JA. Binder removal from ceramics. Annu Rev Mater Sci. 1997;27:147–73. https://doi.org/10.1146/annurev.matsci.27.1.147.
14. Kim HT, Adair JA, Lanagan MT. Thermomechanical behavior of BME capacitors during binder burnout. Am Ceram Soc Bull. 2001;80:34–8.
15. Yoon DH, Lee BI. Processing of barium titanate tapes with different binders for MLCC applications – Part II: comparison of properties. J Europ Ceram Soc. 2004;24:753–61. https://doi.org/10.1016/S0955-2219(03)00334-0.
16. Paik U, Kang KM, Jung YG, Kim J. Binder removal and microstructure with burnout conditions in $BaTiO_3$ based Ni-MLCCs. Ceram Inter. 2003;29:939–46. https://doi.org/10.1016/S0272-8842(03)00049-X.
17. Masia S, Calvert PD, Rhine WE, Kent BH. Effect of oxides on binder burnout during ceramic processing. J Mater Sci. 1989;24:1907–12. https://doi.org/10.1007/BF02385397.
18. Yan H, Roger Cannon W, Shanefield WD. Thermal decomposition behavior of (poly)propylene carbonate). Ceram Inter. 1998;24:433–9. https://doi.org/10.1016/S0272-8842(97)00032-1.
19. Salam LA, Matthews RD, Robertson H. Pyrolysis of polyvinyl butyral (PVB) binder in thermoelectric green tapes. J Europ Ceram Soc. 2000;20:1375–83. https://doi.org/10.1016/S0955-2219(99)00236-8.
20. Seo JJ, Kuk ST, Kim K. Thermal decomposition of PVB (polyvnyl butyral) binder in the matrix and electrolyte of molten carbonate fuel cells. J Power Sourc. 1997;67:61–8. https://doi.org/10.1016/S0378-7753(97)02570-6.
21. "Interactive Ellingham diagram," University of Cambridge. https://www.doitpoms.ac.uk/tlplib/ellingham_diagrams/interactive.php (accessed Apr. 14, 2021)